This is the Pre-Published Version.

The following publication Wang, S., Zhuge, D., Zhen, L., & Lee, C. Y. (2021). Liner Shipping Service Planning Under Sulfur Emission Regulations. Transportation Science, 55(2), 491-509. is available at https://dx.doi.org/10.1287/trsc.2020.1010

Liner shipping service planning under sulfur emission regulations

Shuaian Wang
Department of Logistics & Maritime Studies, The Hong Kong Polytechnic University, Hung Hom, Hong Kong, wangshuaian@gmail.com

Dan Zhuge
Department of Logistics & Maritime Studies, The Hong Kong Polytechnic University, Hung Hom, Hong Kong, dan.zhuge@connect.polyu.hk

Lu Zhen
School of Management, Shanghai University, Shang Da Road 99, Shanghai 200444, China, lzhen@shu.edu.cn

Chung-Yee Lee
Department of Industrial Engineering and Decision Analytics, The Hong Kong University of Science and Technology, Clear Water Bay, Kowloon, Hong Kong, cylee@ust.hk

Air emissions from ships have become an important issue in sustainable shipping because of the low quality of the marine fuel consumed by ships. To reduce sulfur emissions from shipping, the International Maritime Organization has established Emission Control Areas (ECAs) where ships must use low-sulfur fuel with at most 0.1% sulfur or take equivalent emission reduction measures. The use of low-sulfur fuel increases the costs for liner shipping companies and affects their operations management. This study addresses a holistic liner shipping service planning problem that integrates fleet deployment, schedule design, and sailing path and speed optimization, considering the effect of ECAs. We propose a nesting algorithmic framework to address this new and challenging problem. Semi-analytical solutions are derived for the sailing path and speed optimization problem, which are used in the schedule design. A tailored algorithm is applied to solve schedule design problems, and the solutions are used in fleet deployment. The fleet deployment problem is then addressed by a dynamic programming-based pseudo-polynomial time algorithm. Numerical experiments demonstrate that considering the effect of ECAs in liner shipping operations management can reduce over 2% of the costs, which is significant considering that the annual operating cost of a shipping company's network can be as high as several billion dollars.

Key words: Liner shipping operations management; Emission Control Area; Fleet deployment; Schedule design; Ship routing; Dynamic programming

---

1. Introduction

Shipping is the backbone of international trade. The United Nations Conference on Trade and Development (UNCTAD 2019) estimated the global volume of seaborne shipments in 2018 to be 11 billion tons, accounting for over 80% of trade worldwide. These shipments are carried by ocean-going vessels, which burn bunker fuel with a sulfur content of up to 3.5% before 31 December 2019 and 0.5% since 1 January 2020. Zis and Psaraftis (2019) estimated that vessels accounted for 3.5% of global anthropogenic sulfur oxide (SO_x) emissions in 2015[1]. SO_x from shipping causes environmental and health problems, particularly in densely populated coastal areas.

The International Maritime Organization (IMO) and governments around the world have implemented various measures to curb SO_x emissions from shipping, such as limiting the use of high-sulfur fuel when ships are at berth (European Maritime Safety Agency 2017, Hong Kong Environmental Protection Department 2017) and reducing port fees for vessels that use low-sulfur fuel (Maritime and Port Authority of Singapore 2016). The strictest SO_x emission rules are enforced by the IMO in sulfur emission control areas (ECAs), which include the Baltic Sea, the North Sea, the North American region, and the United States Caribbean Sea area, as shown in Figure 1. Ships sailing in ECAs must use fuel with a sulfur content of at most 0.1% or take equivalent measures. The price of marine fuel with a maximum of 0.1% sulfur, e.g., Maritime Gas Oil (MGO)[2], is much higher than that of very low-sulfur fuel oil (VLSFO) which has at most 0.5% of sulfur. Thus, shipping lines must pay a much higher fuel bill than before[3]. An alternative approach to complying with the ECA rules is to use SO_x scrubbers, which are onboard exhaust gas cleaning systems (EGCS) that remove SO_x from ships' exhaust gases by chemical reaction. Ships equipped with scrubbers can still burn high-sulfur fuel oil (HSFO) which has at most 3.5% of sulfur, but the average installation cost is as high as US$2.5 million (Bockmann 2020).

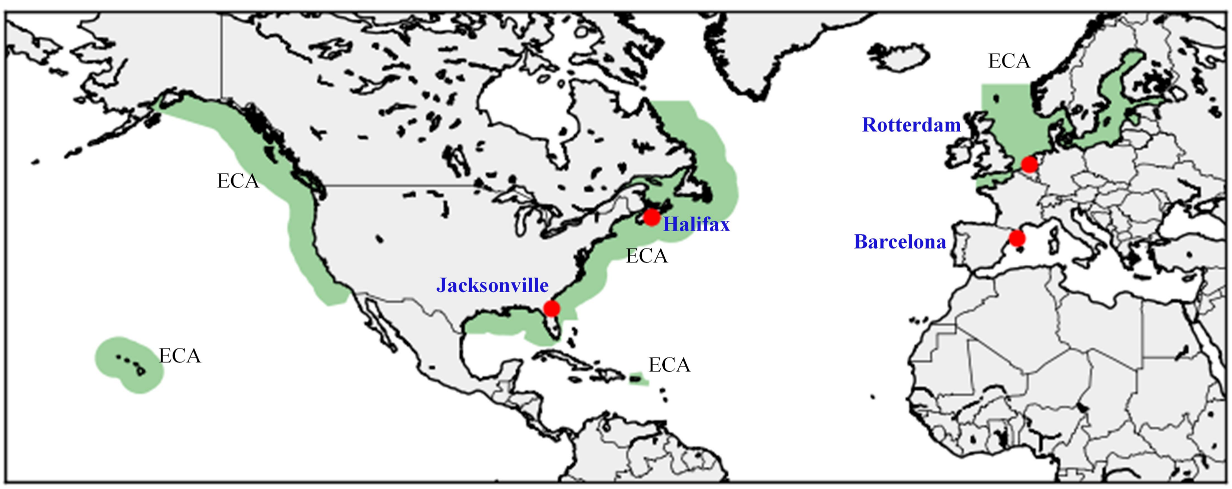

Figure 1 ECAs designated by the IMO

[1] This proportion will significantly be lower since 2020 because of the more strict sulfur limit on marine fuel starting from 1 January 2020

[2] Ships that burn other types of clean fuel rather than MGO, such as liquefied natural gas, are also allowed to sail in ECAs.

[3] For example, Maersk Line spent around US$300 million a year to comply with ECA rules (Hand 2015) when the maximum sulfur content of marine fuel outside ECAs was 3.5%.

The focus of this study is on liner shipping operations management that considers ECAs. We first discuss the following key terms used in liner shipping.

(i) **Route**: As shown in Figure 2, a liner route has a fixed sequence of ports of call, similar to a bus route. The ports of call on a route form a loop, which means ships visit the first again after visiting the last. A liner shipping company operates a number of liner routes.

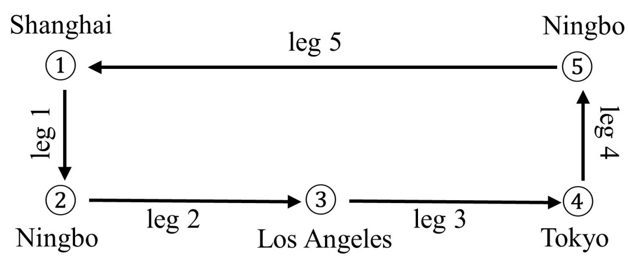

Figure 2 **A liner route**

(ii) **Leg**: The sailing from one port of call to the next is called a leg. A route consists of two or more legs.

(iii) **Trajectory (path)**: Ships sailing on the same leg may follow different trajectories (also called paths), as shown in Figure 3. A navigable path on a leg must meet a number of requirements, for instance, there must be no obstacles (e.g., islands) along it and the water along the path must be sufficiently deep. A scrubber-equipped ship always sails along the shortest navigable path. A traditional ship (without scrubbers) may follow a navigable path that may not be the shortest in total but whose distance within ECAs is the shortest.

(iv) **Fuel consumption rate**: the fuel consumption rate (ton/nautical mile, or ton/nm) of a ship is a convex increasing function of the sailing speed (Notteboom and Vernimmen 2009, Fagerholt and Psaraftis 2015). Therefore, when a traditional ship sails along a path that crosses the boundary of an ECA, its speed within the ECA should be lower than when outside the ECA; this speed differentiation saves fuel costs by burning less MGO within the ECA, which is more expensive than VLSFO burned outside the ECA.

(v) **Weekly service frequency**: Each route provides a weekly service frequency, that is, each port of call is visited on the same day every week. This frequency is achieved by deploying a string of ships on each route and the number of ships in the string is equal to the round-trip journey time (unit: week), defined as the duration between two consecutive visits at the first port of call. For example, if the round-trip journey time is three weeks, then three ships must be deployed to provide a weekly service frequency; if the average sailing speed of the ships increases and the round-trip journey time is reduced to two weeks, then only two ships will be deployed to maintain the frequency.

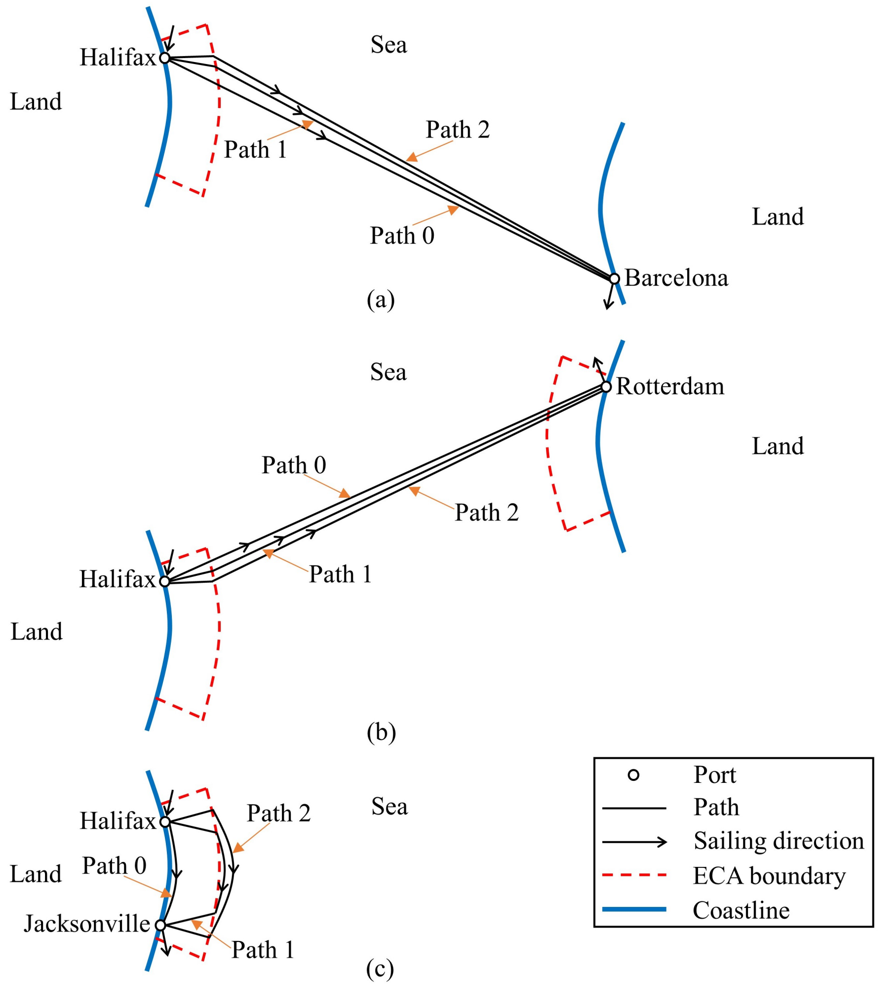

Figure 3 **Navigable paths for the sailings from Halifax to Barcelona, Rotterdam, and Jacksonville**

We examine the joint fleet deployment, schedule design, and path and speed optimization decisions for a liner shipping company that operates a set of liner routes with fixed sequences of ports of call.

(i) **The fleet deployment decision faced by the company is how many of each type of ship to deploy on each liner route**. The fixed cost of a scrubber-equipped ship is higher than that of a traditional ship, but it burns HSFO, which is cheaper than VLSFO and MGO. As the company has a finite number of ships of each type in its fleet, the assignment of ships to different routes must be examined holistically. The fuel costs of a route are related to the numbers of ships of each type deployed. Deploying more ships on a route means the round-trip journey time will be longer because of the weekly service frequency, and the fuel consumption will be lower because of the lower average sailing speed. Therefore, the fixed costs of ships and the fuel costs must be balanced in fleet deployment.

(ii) The exact fuel costs of a route, which are the total fuel costs of all the legs of the route, depend on the **schedule design, which establishes the sailing time of each leg**. In other words, schedule design allocates the total sailing time of the route (the round-trip journey time minus the total time spent at ports) to its legs. The optimal allocation depends on the sensitivity of the fuel consumption of each leg to its sailing time. Different types of ships must follow the same schedule if they are operated on the same route.

(iii) The relation between fuel consumption of a leg and its sailing time can be obtained by **optimizing the sailing paths and speeds of ships**, that is, given a set of navigable paths for the leg, identifying the one with the lowest fuel cost and deciding the speed on the path within ECAs and the speed on the path outside ECAs for each type of ship.

This study addresses a holistic liner shipping service planning problem that integrates fleet deployment, schedule design, and path and speed optimization in which the effect of ECAs is considered. The ECA rules result in a fleet of different types of ships being operated by shipping companies, including traditional ships and scrubber-equipped ships, and the rules also lead to the path and speed optimization for traditional ships. We integrate the use of different types of ships, and path and speed optimization under the ECA rules, into the traditional fleet deployment and schedule design problem. The interlinked decisions of fleet deployment, schedule design, and path and speed optimization complicate the problem. We propose a nesting algorithmic framework to address this new and challenging problem, and find that deploying multiple types of ships on one route is generally undesirable. The methodology proposed in this study can help liner operations managers develop optimal liner service plans under ECA regulations. Extensive numerical experiments have demonstrated that incorporating the effect of ECA rules into liner shipping service planning decisions can save over 2% of the costs, and as the annual operating cost of a shipping company's network can be up to several billion dollars, this is a significant amount, particularly due to the low profit margins (UNCTAD 2018). For example, the largest container shipping company, Maersk Line, had a profit margin of 3.2% in 2017 (Maersk 2017). Under the dual pressure of the long-term market downturn and the increasingly stringent environmental regulations on shipping, global shipping companies urgently need to optimize their shipping services to improve efficiency, reduce cost, and enhance competitiveness (UNCTAD 2018).

The remainder of the paper is organized as follows. The related literature is reviewed in Section 2. Section 3 presents the algorithmic framework. Section 4 addresses the path and speed optimization problem for traditional ships which switch to MGO when entering ECAs. Section 5 elaborates the schedule design problem. In Section 6, the fleet deployment problem is solved. Section 7 reports the computational results. The conclusions are presented in the last section. The proofs of lemmas, propositions, and theorems with the exception of Proposition 4 are presented in §EC.1.

2. Literature Review

Routing and scheduling problems are key concerns in the operations management of shipping (Christiansen et al. 2004, ?, 2013, Fransoo and Lee 2013, Meng et al. 2014, ?, ?, Lee and Song 2017) and land transportation (Cordeau et al. 1998, Legros et al. 2019). In this section, we describe how our work is related to the following areas of study: (i) fleet management and scheduling, (ii) sailing path and speed optimization, (iii) sustainable shipping operations management, and (iv) multi-stage decision making.

Liner ship fleet deployment problems have been extensively studied in the literature. They are mainly formulated as mixed-integer linear programs and solved by optimization solvers (Meng and Wang 2011, Ng 2014). Wang and Wang (2016) examined the deployment of a fleet of identical ships and proposed a polynomial-time bi-section search-based algorithm, which takes advantage of the convexity of the fuel cost of a liner route in the number of ships deployed. Under the ECA rules, shipping companies operate both traditional and scrubber-equipped ships. Traditional ships may follow a longer path to reduce fuel costs, and as will be shown in Section 6, the fuel cost of a route is no longer convex in the number of ships deployed. We propose a dynamic programming-based pseudo-polynomial time algorithm for the deployment of multiple types of ships. Liner route schedule design problems are often solved by exact algorithms that take advantage of the convexity of fuel cost functions of speed (Hvattum et al. 2013, Wang 2016). These algorithms are not applicable to our problem because, as will be shown in Section 4, the fuel cost functions are in general non-convex and discontinuous under ECA rules. In the context of ECAs, multiple types of ships are deployed on one route and they follow the same schedule, which contrasts with the heterogeneous fleet settings in vehicle routing problems (Baldacci et al. 2008), surface and air shipments of humanitarian goods (Park et al. 2018), and planning the number of advanced life support and basic life support ambulances in emergency medical service systems (Chong et al. 2015).

The literature on sailing path and speed optimization between two ports has mainly focused on weather routing, that is, determining the sailing path that minimizes the fuel consumption or minimizes the sailing time while considering different weather conditions at different locations at sea (Perakis and Papadakis 1989, Papadakis and Perakis 1990, Lo and McCord 1998). The sailing path is usually determined by dynamic programming approaches over discretized longitudes and latitudes of the sea. Like those for sailing paths, Chen and Solak (2015) proposed an optimized profile descent procedure for aircraft landing that reduces fuel consumption compared with the conventional stair-step approach. The above weather routing and aircraft landing settings, however, only include one type of fuel. In contrast, the ECA rules mandate the switch of fuel before a traditional ship enters an ECA. Doudnikoff and Lacoste (2014), Fagerholt et al. (2015), and Fagerholt and Psaraftis (2015) contributed fundamental breakthroughs in ship routing and scheduling under ECA rules and developed numerical algorithms to compute the speeds within and outside the ECAs. We complement these studies by deriving analytical properties that shed light into the trade-off associated with sailing distances within and outside ECAs.

Air emissions from ships are an important issue in the sustainable operations management of liner shipping. Shipping air emission reduction measures have been widely discussed (**???**). We pay attention to the after-treatment technology, scrubbers, which is closely related to this study. Jiang et al. (2014) and Zis et al. (2016) performed a net present value analysis to examine whether a ship that often sails within ECAs should install a scrubber. They focused on one ship whose speed and path are assumed to be fixed before and after installing the scrubber. Abadie et al. (2017) also conducted a net present value analysis to compare whether a ship should install a scrubber or switch to MGO within ECAs. They considered factors such as spot and future fuel prices, the time that the ship sails within ECAs, the remaining lifespan of the ship, and the cost of scrubber installation. Gu and Wallace (2017) investigated factors that affect the economic viability of retrofitting traditional ships with scrubbers. They considered a route with a fixed schedule that is serviced by a traditional ship. This ship will follow an optimized path and speeds on each leg of the route to minimize the total fuel costs, instead of sailing along the shortest navigable path at the average speed. If the traditional ship is retrofitted with scrubbers, the resulting scrubber-equipped ship will sail along the shortest navigable path at the average speed, burning HSFO. The traditional ship should thus be retrofitted with scrubbers if the fuel cost difference between it adhering to the optimized path and speeds and the scrubber-equipped ship is greater than the retrofitting cost. They concluded that the benefit of retrofitting a traditional ship with scrubbers without considering that the ship may optimize its path and speeds is likely to be significantly overestimated, and the overestimation is less severe when the density of ports of call inside ECAs is higher. As the schedule of the route is fixed, Gu and Wallace (2017) has essentially addressed the path and speed optimization problem numerically. Building on their work, we derive semi-analytical results for the path and speed optimization problem and further consider the joint fleet deployment, schedule design, and sailing path and speed optimization problem for multiple routes, and that multiple types of ships can be deployed on each of them.

Multi-stage models are often used for problems in which decisions are made in each period of a multi-period horizon (Papageorgiou et al. 2014), in which decisions are made both before and after uncertain factors are realized and observed (Mak et al. 2013), and in which decisions are in neither of the above categories but can still be decomposed into several stages, such as in multi-echelon inventory management (Angelus and Zhu 2017). The holistic planning problem in this paper belongs to this final category because it consists of three stages of decisions: fleet deployment (stage 1), schedule design (stage 2), and sailing path and speed optimization (stage 3). Unlike most multi-stage decision problems, the problem in this study has the nice properties that the decision process in stage 1 includes many *independent* decision processes in stage 2 and a decision process in stage 2 includes many *independent* decision processes in stage 3. Based on these two properties, we can design a nesting algorithmic framework.

3. Modeling and algorithmic framework

In this section, we first describe the joint fleet deployment, schedule design, and path and speed optimization problem considering ECAs. We then formulate a mathematical model for the problem. Finally, a nesting algorithmic framework is proposed. The main notation used in the paper is listed below.

Sets, parameters and known functions

R	Total number of liner routes
I_r	Total number of ports of call on liner route r, which is equal to the total number of legs on the route
P_{ri}	Set of navigable paths for leg i of liner route r
K	Set of types of ships to deploy on the routes
K_1	Set of types of ships that consume different types of fuel within and outside ECAs
K_2	Set of types of ships that consume the same type of fuel within and outside ECAs; $K_1 \cup K_2 = K$
$\mathbb{Z}_+$	Set of nonnegative integers
α_k^E	Price (US\$/ton) of fuel consumed within ECAs by type-k ships, $k \in K$
α_k^N	Price (US\$/ton) of fuel consumed outside ECAs by type-k ships, $k \in K$
Δ	Unit time (hour) for sailing time discretization in schedule design
a_{kri}, b_{kri}	Conversion factors between fuel consumption per unit distance and sailing speed of ships: fuel consumption rate (ton/nm) of a type-k ship sailing on leg i of route r is $a_{kri} \cdot \text{speed}^{b_{kri}}$
c_k	Fixed cost (US\$/week) of a ship of type $k \in K$
Γ_{ri}	Time (hours) spent at the ith port of call on liner route r
Γ_r	Total time (hours) spent at all ports of call on liner route r; $\Gamma_r := \sum_{i=1}^{I_r} \Gamma_{ri}$
L_{rip}^E	Sailing distance (nm) within ECAs on path $p \in P_{ri}$ of leg i of liner route r
L_{rip}^N	Sailing distance (nm) outside ECAs on path $p \in P_{ri}$ of leg i of liner route r
$L_{ri}^{\min}$	Total sailing distance (nm) of the shortest navigable path for leg i of liner route r; $L_{ri}^{\min} := \min_{p \in P_{ri}} (L_{rip}^E + L_{rip}^N)$
W	Number of hours in a week, $W = 168$ (hours/week)
$m_r^{\min}$	Minimum number of ships required to be deployed on liner route r; $m_r^{\min} = \lceil (\Gamma_r + \sum_{i=1}^{I_r} t_{ri}^{\min})/W \rceil$

Q_k	Number of ships of type $k \in K$ in the fleet
$V^{\max}$	Maximum sailing speed (knots) of a ship
$t_{rip}^{\min}$	Minimum sailing time (hours) on path $p \in P_{ri}$ of leg i of liner route r; $t_{rip}^{\min} = (L_{rip}^E + L_{rip}^N)/V^{\max}$
$t_{ri}^{\min}$	Minimum sailing time (hours) on leg i of liner route r; $t_{ri}^{\min} = L_{ri}^{\min}/V^{\max} = \min_{p \in P_{ri}} t_{rip}^{\min}$
$\lceil x \rceil$	Smallest integer greater than or equal to x
$\lfloor x \rfloor$	Largest integer smaller than or equal to x.

Decision variables and values to be calculated

m_{kr}	Number of ships of type $k \in K$ deployed on liner route r
$\mathbf{m}_r$	Vector of m_{kr}, $k \in K$, for route r
$\mathbf{m}$	Vector of $\mathbf{m}_r$, $r = 1, ..., R$
$C_r(\mathbf{m}_r)$	Minimum fuel cost (US\$/week) of liner route r when m_{kr} ships of type $k \in K$ are deployed on the route
t_{ri}	Sailing time (hours) on leg i of liner route r
$\mathbf{t}_r$	Vector of t_{ri}, $i = 1, ..., I_r$, for route r
$c_{kri}(t_{ri})$	Minimum fuel cost function for a ship of type $k \in K$ that sails on leg i of liner route r with sailing time t_{ri}
$g_{krip}(t_{ri})$	Minimum fuel cost function for a ship of type $k \in K$ that sails on path $p \in P_{ri}$ of leg i of liner route r with sailing time t_{ri}
v_{krip}^E	Sailing speed (knots) of a ship of type $k \in K$ within ECAs on path $p \in P_{ri}$ of leg i of liner route r
v_{krip}^N	Sailing speed (knots) of a ship of type $k \in K$ outside ECAs on path $p \in P_{ri}$ of leg i of liner route r
z_{krip}	Binary variable, equal to one if ships of type $k \in K$ sail on path $p \in P_{ri}$ of leg i of liner route r, and zero otherwise.

A liner shipping company operates a total of R routes. Route $r = 1, ..., R$ has I_r ports of call. For example, the route in Figure 2 has five ports of call. Route r has I_r legs, in which leg $i = 1, ..., I_r$ is the sailing from the ith port of call to the $(i+1)$th (the (I_r+1)th port of call is defined as the 1st one). Note that index $i = 1, ..., I_r$ is used to refer to either a port of call or a leg. A set of navigable paths, denoted by P_{ri}, is given for leg $i = 1, ..., I_r$ of route $r = 1, ..., R$, as shown in Figure 3. The distances of path $p \in P_{ri}$ within and outside ECAs are L_{rip}^E and L_{rip}^N (nm), respectively (the superscript "E" means "ECA" and "N" means "non-ECA"). The shortest navigable path for leg i of route r has a total sailing distance denoted by $L_{ri}^{\min} := \min_{p \in P_{ri}} (L_{rip}^E + L_{rip}^N)$. The sailing time on leg i of route r, denoted by t_{ri}, is to be designed by the shipping company. Once a ship arrives at the ith port of call on liner route r, it will stay there for Γ_{ri} (hours) to allow cargo to be loaded and unloaded, and it will then sail to the next port of call. Define $\Gamma_r = \sum_{i=1}^{I_r} \Gamma_{ri}$ as the total port time of route r. We assume fixed time Γ_{ri} is spent at each port of call but our model can also handle random port times, which will be discussed in Section 4.3.

In view of the ECA rules, the company operates a fleet of different types of ships that can be deployed on the R routes. The set of ship types is denoted by K. The number of type-k ships in the fleet is Q_k, $k \in K$. A type-k ship has a weekly fixed cost c_k. We assume all ships have the same maximum sailing speed $V^{\max}$ (knots)[4]; hence, the minimum sailing time (hours) by a ship on path $p \in P_{ri}$ of leg i of liner route r is $t_{rip}^{\min} = (L_{rip}^E + L_{rip}^N)/V^{\max}$ and the minimum sailing time on leg i is $t_{ri}^{\min} = L_{ri}^{\min}/V^{\max} = \min_{p \in P_{ri}} t_{rip}^{\min}$. The fuel consumption rate (ton/nm) of a type-k ship sailing on leg i of route r is a convex power function of speed $a_{kri} \cdot v^{b_{kri}}$, where $a_{kri} > 0$ and $b_{kri} > 1$ are parameters and v (knots) is the sailing speed (Notteboom and Vernimmen 2009, Fagerholt et al. 2010, Ronen 2011, Wang and Meng 2012). The prices of fuel consumed within and outside ECAs by type-k ships are represented by α_k^E and α_k^N (US\$/ton), respectively. $\alpha_k^E \geq \alpha_k^N$, and they are the same for scrubber-equipped ships. When multiple types of ships are deployed on a route r, they must follow the same schedule, that is, they have the same sailing time t_{ri} on each leg $i = 1, ..., I_r$, whereas they may follow different paths to save fuel costs.

Ship deployment on the R liner routes, i.e., the number of type-k ships to deploy on route $r = 1, ..., R$, denoted by m_{kr}, is a tactical decision. Once a ship is deployed on a route, it will operate on it for three to six months. The decisions on the number of ships to deploy and the sailing speeds of the ships must ensure each route provides a weekly service frequency. This means each port of call on the route is visited on the same day every week (but it may be visited by different ships) and the headway between two consecutive ships is one week. We define $W = 168$ (hours/week). Given a total of $\sum_{k \in K} m_{kr}$ ships deployed on route r, the speeds of the ships must guarantee that the round-trip journey time is $\sum_{k \in K} m_{kr}$ weeks ($W \cdot \sum_{k \in K} m_{kr}$ hours). The round-trip journey time of route $r = 1, ..., R$ is the sum of the port time Γ_r on the route and the total sailing time on all of the legs. The minimum number of ships required to be deployed on route r, denoted by $m_r^{\min}$, can be derived by $m_r^{\min} = \lceil (\Gamma_r + \sum_{i=1}^{I_r} t_{ri}^{\min})/W \rceil$, where $\lceil x \rceil$ returns the smallest integer not less than x.

The objective of the overall planning problem is to minimize the total average cost per week of all routes, which consists of the fixed costs of ships and the fuel costs[5]. Reducing the fuel costs means reducing the sailing speed, which increases the round-trip journey time and requires more ships to be deployed, and vice versa. Therefore, the overall planning problem is to balance the trade-off

[4] We make this assumption to simplify the notation. If different maximum sailing speeds $V_k^{\max}$ for different types of ships $k \in K$ are considered, we can define $V^{\max} := \max\{V_k^{\max}, k \in K\}$ and the fuel consumption per unit distance by a ship of type $k \in K$ is infinity when its speed is greater than $V_k^{\max}$ and smaller than or equal to $V^{\max}$.

[5] The fuel costs of a route in different weeks may be different when multiple types of ships are deployed on it. Therefore, we minimize the total *average* cost per week of all routes.

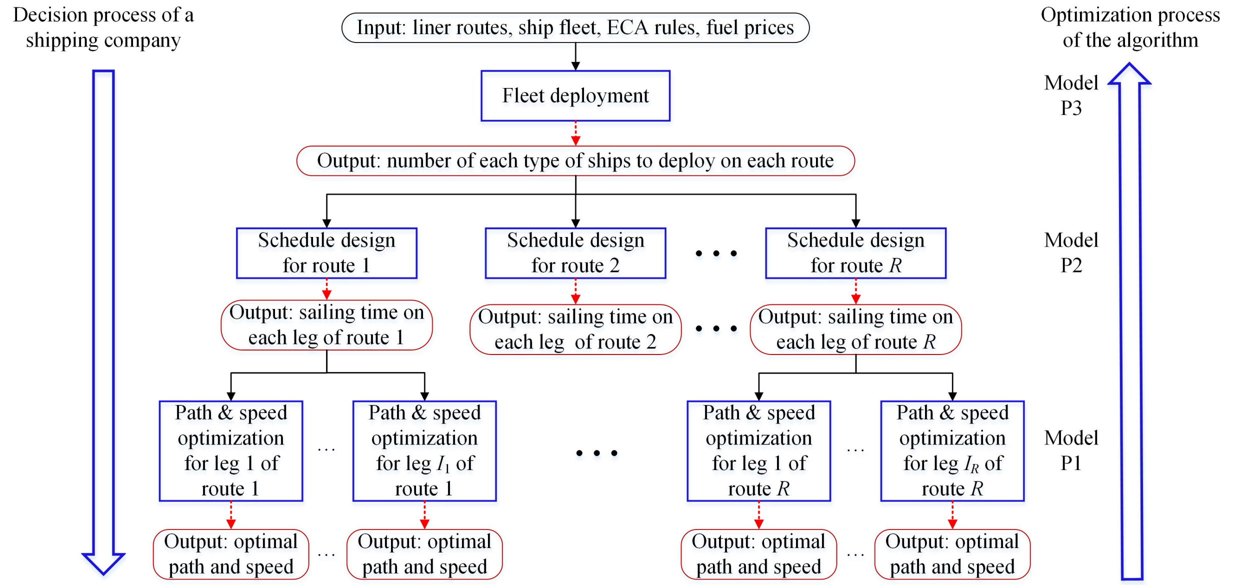

Figure 4 **Framework of the decisions of the joint fleet deployment, schedule design, and path and speed optimization problem considering ECAs**

between fuel costs and the fixed costs of ships. The decisions of the joint problem are shown in Figure 4. The company first makes the fleet deployment decisions, represented by vector $\mathbf{m}$. The fixed costs of ships depend on the number of ships of each type deployed on the R routes. The fuel costs depend on the schedule design and path and speed optimization decisions. For each route $r = 1, ..., R$, given fleet deployment decision $\mathbf{m}_r$, the company designs the schedule, that is, the sailing time on every leg $i = 1, ..., I_r$, denoted by t_{ri}. Once the sailing time vector $\mathbf{t}_r$ is determined, the company makes decisions for each type of ship regarding its optimal sailing path and optimal speeds within and outside the ECAs on the sailing path, to minimize the fuel cost for the leg. To formulate path and speed optimization decisions, we denote z_{krip} as a 0–1 variable that equals 1 if and only if type-k ships sail on path $p \in P_{ri}$ of leg i of route r. We define continuous variables v^E_{krip} and v^N_{krip} that represent the speeds of type-k ships within and outside ECAs on the path, respectively.

3.1. Model

The joint planning problem can be formulated as

$$
\begin{aligned}
[\text{P0}] \quad \min \quad & \sum_{r=1}^{R} \Bigg\{ \sum_{k \in K} c_k \cdot m_{kr} \\
& + \sum_{k \in K} \frac{m_{kr}}{\sum_{k' \in K} m_{k'r}} \underbrace{\sum_{i=1}^{I_r} \sum_{p \in P_{ri}} \left[\alpha^E_k L^E_{rip} a_{kri} \cdot (v^E_{krip})^{b_{kri}} + \alpha^N_k L^N_{rip} a_{kri} \cdot (v^N_{krip})^{b_{kri}} \right] z_{krip}}_{\text{total fuel cost for a ship of type } k \text{ to complete a round-trip journey of route } r} \Bigg\}
\end{aligned} \tag{1}
$$

subject to

$$\Gamma_r + \sum_{i=1}^{I_r} t_{ri} = W \cdot \sum_{k\in K} m_{kr}, \quad r = 1, ..., R \tag{2}$$

$$\sum_{p\in P_{ri}} z_{krip} = 1, \quad r = 1, ..., R, \ i = 1, ..., I_r, \ k \in K \tag{3}$$

$$\sum_{p\in P_{ri}} \left(\frac{L^E_{rip}}{v^E_{krip}} + \frac{L^N_{rip}}{v^N_{krip}} \right) z_{krip} = t_{ri}, \quad r = 1, ..., R, \ i = 1, ..., I_r, \ k \in K \tag{4}$$

$$\sum_{r=1}^{R} m_{kr} \le Q_k, \ k \in K \tag{5}$$

$$\sum_{k\in K} m_{kr} \ge m^{\min}_r, \quad r = 1, ..., R \tag{6}$$

$$z_{krip} \in \{0, 1\}, \quad r = 1, ..., R, \ i = 1, ..., I_r, p \in P_{ri}, \ k \in K \tag{7}$$

$$0 < v^E_{krip}, v^N_{krip} \le V^{\max}, \quad r = 1, ..., R, \ i = 1, ..., I_r, p \in P_{ri}, \ k \in K \tag{8}$$

$$t_{ri} \ge t^{\min}_{ri}, \quad r = 1, ..., R, \ i = 1, ..., I_r \tag{9}$$

$$m_{kr} \in \mathbb{Z}_+, \quad r = 1, ..., R, \ k \in K, \tag{10}$$

where $\mathbb{Z}_+$ denotes the set of nonnegative integers. The objective function (1) minimizes the total average cost per week of all the R routes, which includes the fixed costs of ships and fuel costs. When m_{kr} ships of type $k \in K$ are deployed on route r to provide a weekly service frequency, the round-trip journey time is equal to $\sum_{k\in K} m_{kr}$ weeks. In a period of $\sum_{k\in K} m_{kr}$ consecutive weeks, a deployed ship will sail on all the legs of route r; hence, the average fuel cost per week for one type-k ship on route r is $\frac{1}{\sum_{k'\in K} m_{k'r}} \sum_{i=1}^{I_r} \sum_{p\in P_{ri}} \left[\alpha^E_k L^E_{rip} a_{kri} \cdot (v^E_{krip})^{b_{kri}} + \alpha^N_k L^N_{rip} a_{kri} \cdot (v^N_{krip})^{b_{kri}} \right] z_{krip}$. Given that m_{kr} ships of type $k \in K$ are deployed on route r, the average fuel cost per week of route r is $\sum_{k\in K} \frac{m_{kr}}{\sum_{k'\in K} m_{k'r}} \sum_{i=1}^{I_r} \sum_{p\in P_{ri}} \left[\alpha^E_k L^E_{rip} a_{kri} \cdot (v^E_{krip})^{b_{kri}} + \alpha^N_k L^N_{rip} a_{kri} \cdot (v^N_{krip})^{b_{kri}} \right] z_{krip}$. Eqs. (2) ensure that the number of ships deployed on each route can provide a weekly service frequency: the round-trip journey time (hour) $W \cdot \sum_{k\in K} m_{kr}$ is equal to the sum of the fixed total port time Γ_r and the total sailing time $\sum_{i=1}^{I_r} t_{ri}$. Eqs. (3) require that exactly one path for each leg is chosen for each type of ship. Eqs. (4) ensure that all types of ships have the same sailing schedule, i.e., the same sailing time t_{ri} on each leg. Constraints (5) define the maximum number of each type of ship that can be used. Constraints (6) enforce a minimum number of $m^{\min}_r$ ships deployed on route r. Note that Constraints (6) are redundant for model [P0] due to Constraints (2), however, they will be useful when we break down model [P0] into submodels. Constraints (7) define z_{krip} as binary variables. Constraints (8) define the sailing speeds as nonnegative variables with the upper bound $V^{\max}$. Constraints (9) define t_{ri} as continuous variables and their lower bounds. Constraints (10) define m_{kr} as nonnegative integer variables.

3.2. Algorithmic framework

The joint fleet deployment, schedule design, and path and speed optimization problem has the following nice properties. First, the decisions for different routes are coupled only by Constraints (5). Once the value of $\mathbf{m}$ is determined, the problem can be decomposed for each route. Specifically, for a route r, the design of its schedule $\mathbf{t}_r$ solely depends on $\mathbf{m}_r$ and is independent of the decisions for the other routes. Second, the decisions for different legs of a route r are coupled only by Constraints (2). Once schedule $\mathbf{t}_r$ is determined, the optimal path and speed optimization decision for leg i of route r is independent of the decisions for the other legs.

Thus, we can design a nesting algorithmic framework, which proceeds in the *opposite* direction to the decision process shown in Figure 4. We first examine the **path and speed optimization** problem for ships sailing on leg i of route r. We represent by $c_{kri}(t_{ri})$ the minimum fuel cost function for a type-k ship that sails on leg i of route r with sailing time t_{ri}, $t_{ri} \geq t_{ri}^{\min}$, $k \in K$. Let K_1 be the set of types of ships that consume different types of fuel within and outside ECAs, and K_2 be the set of types of ships that consume the same type of fuel within and outside ECAs; $K_1 \cup K_2 = K$. The fuel consumption rate of a ship is a convex function of speed, so a ship of type $k \in K_2$, e.g., a scrubber-equipped ship, simply sails along the shortest navigable path at the average speed (Hvattum et al. 2013); therefore,

$$c_{kri}(t_{ri}) = \alpha_k^N L_{ri}^{\min} a_{kri} \cdot \left(\frac{L_{ri}^{\min}}{t_{ri}}\right)^{b_{kri}}, \quad t_{ri} \geq t_{ri}^{\min}, \qquad k \in K_2. \tag{11}$$

To calculate $c_{kri}(t_{ri})$ for a ship of type $k \in K_1$, for example a traditional ship, we first define $g_{krip}(t_{ri})$ as the minimum fuel cost for a ship of type $k \in K_1$ to sail on path $p \in P_{ri}$ of leg i of route r with sailing time t_{ri}, $t_{ri} \geq t_{ri}^{\min}$. For each $p \in P_{ri}$, we define v_{krip}^E and v_{krip}^N as the decision variables representing the speeds within and outside ECAs, respectively. Then,

$$g_{krip}(t_{ri}) = \min \left[\alpha_k^E L_{rip}^E a_{kri} \cdot (v_{krip}^E)^{b_{kri}} + \alpha_k^N L_{rip}^N a_{kri} \cdot (v_{krip}^N)^{b_{kri}}\right] \tag{12}$$

subject to

$$\frac{L_{rip}^E}{v_{krip}^E} + \frac{L_{rip}^N}{v_{krip}^N} = t_{ri} \tag{13}$$

$$0 < v_{krip}^E, v_{krip}^N \leq V^{\max}. \tag{14}$$

The value of $c_{kri}(t_{ri})$, $k \in K_1$, $t_{ri} \geq t_{ri}^{\min}$, can then be obtained by the following **path and speed optimization model**, which optimizes the choice of path and the speed within ECAs and the speed outside ECAs on the chosen path:

$$\text{[P1]} \quad c_{kri}(t_{ri}) = \min_{p \in P_{ri}} g_{krip}(t_{ri}), \quad t_{ri} \geq t_{ri}^{\min}, \quad k \in K_1. \tag{15}$$

The solution to [P1] is elaborated in Section 4.

The results of $c_{kri}(t_{ri})$ for legs $1,...,I_r$ and ship types $k\in K$ are then treated as input for the schedule design problem for each route $r=1,...,R$, which aims to find the $\mathbf{t}_r$ that minimizes the fuel costs for the route. We denote by $C_r(\mathbf{m}_r)$ the minimum average fuel costs of route r per week when the number of type-k ships deployed on it is m_{kr}, $k\in K$. Given $\mathbf{m}_r$, we formulate the following **schedule design model** for route r:

$$[\text{P2}]\quad C_r(\mathbf{m}_r)=\min\sum_{k\in K}\frac{m_{kr}}{\sum_{k'\in K}m_{k'r}}\sum_{i=1}^{I_r}c_{kri}(t_{ri}) \tag{16}$$

subject to

$$\Gamma_r+\sum_{i=1}^{I_r}t_{ri}=W\cdot\sum_{k\in K}m_{kr} \tag{17}$$

$$t_{ri}\geq t_{ri}^{\min},\quad i=1,...,I_r. \tag{18}$$

The solution to [P2] is elaborated in Section 5.

The outcomes of $C_r(\mathbf{m}_r)$ for all the routes $r=1,...R$ and all possible values of $\mathbf{m}_r$ will be the input for the fleet deployment. The fleet deployment problem minimizes the total average cost per week (the sum of fixed costs of ships and fuel costs) of all routes by deciding the number of ships of each type k to deploy on each route r, denoted by $m_{kr}, r=1,...,R, k\in K$. We formulate the following **fleet deployment model**:

$$[\text{P3}]\quad \min\sum_{r=1}^{R}\left[\sum_{k\in K}c_k\cdot m_{kr}+C_r(\mathbf{m}_r)\right] \tag{19}$$

subject to Constraints (5), (6) and (10). The solution to model [P3] is elaborated in Section 6.

4. Path and speed optimization model [P1]

In this section, the path and speed optimization model [P1] is examined. We discuss the solution for model (12) in Section 4.1 and the solution for model [P1] in Section 4.2. We extend the models to account for random port times in Section 4.3.

4.1. Speed optimization model for a given path

To characterize the function $g_{krip}(t_{ri})$ in Eq. (12) for a navigable path $p\in P_{ri}$ and a particular ship type $k\in K_1$, we define two critical values of t_{ri} as follows.

The first critical value is the smallest feasible value, which is denoted by $t_{rip}^{\min}$ and is achieved when the ship sails at $V^{\max}$ both within and outside ECAs, i.e.,

$$t_{rip}^{\min}=\frac{L_{rip}^{E}+L_{rip}^{N}}{V^{\max}}. \tag{20}$$

The domain of $g_{krip}(t_{ri})$ is $[t_{rip}^{\min}, \infty)$.

For the second critical value, denoted by $\hat{t}_{krip}$, the constraints $v_{krip}^E \le V^{\max}$ and $v_{krip}^N \le V^{\max}$ in (14) are unbinding if and only if $t_{ri} > \hat{t}_{krip}$. To calculate $\hat{t}_{krip}$, we first define a coefficient:

Definition 1. *Given the ship fuel consumption parameter b_{kri} and the fuel prices α_k^E and α_k^N,*

$$\gamma_{kri} := \left(\frac{\alpha_k^E}{\alpha_k^N}\right)^{\frac{1}{1+b_{kri}}} \tag{21}$$

is called the "conversion coefficient" and $\gamma_{kri} L_{rip}^E + L_{rip}^N$ is called the "converted" non-ECA distance of path p for type-k ships.

The value of $\hat{t}_{krip}$ is the ratio of the converted non-ECA distance of the path and the maximum speed:

$$\hat{t}_{krip} = \frac{\gamma_{kri} L_{rip}^E + L_{rip}^N}{V^{\max}}. \tag{22}$$

We denote by v_{krip}^{E*} and v_{krip}^{N*} the optimal speeds within and outside ECAs, respectively, for model (12). Then,

Proposition 1. *When $t_{ri} \in (\hat{t}_{krip}, \infty)$,*

$$v_{krip}^{E*} = \frac{L_{rip}^E + \frac{1}{\gamma_{kri}} L_{rip}^N}{t_{ri}} \tag{23}$$

$$v_{krip}^{N*} = \frac{\gamma_{kri} L_{rip}^E + L_{rip}^N}{t_{ri}} \tag{24}$$

$$\frac{v_{krip}^{E*}}{v_{krip}^{N*}} = \frac{1}{\gamma_{kri}}; \tag{25}$$

when $t_{ri} \in [t_{rip}^{\min}, \hat{t}_{krip}]$,

$$v_{krip}^{E*} = \frac{L_{rip}^E}{t_{ri} - \frac{L_{rip}^N}{V^{\max}}} \tag{26}$$

$$v_{krip}^{N*} = V^{\max}. \tag{27}$$

Eq. (25) shows that when $t_{ri} > \hat{t}_{krip}$, $v_{krip}^{E*} < v_{krip}^{N*}$ as $\gamma_{kri} > 1$; for example, if $b_{kri} = 2$ and $\alpha_k^E = 2\alpha_k^N$, then $v_{krip}^{E*} \approx 0.8 v_{krip}^{N*}$. Eq. (27) shows that when $t_{ri} \le \hat{t}_{krip}$, $v_{krip}^{E*} \le v_{krip}^{N*}$ ($v_{krip}^{E*} = v_{krip}^{N*}$ only when $t_{ri} = t_{rip}^{\min}$). Therefore, the ship should slow down within ECAs to save fuel costs.

We have the following property for model (12):

Proposition 2. *$g_{krip}(t_{ri})$ is a two-piece continuous function:*

$$g_{krip}(t_{ri}) = \begin{cases} \alpha_k^E \cdot a_{kri} \cdot (t_{ri} - \frac{L_{rip}^N}{V^{\max}})^{-b_{kri}} \cdot (L_{rip}^E)^{1+b_{kri}} + \alpha_k^N \cdot L_{rip}^N \cdot a_{kri} \cdot (V^{\max})^{b_{kri}}, & t_{rip}^{\min} \le t_{ri} \le \hat{t}_{krip} \\ \alpha_k^N \cdot a_{kri} \cdot (t_{ri})^{-b_{kri}} \cdot (\gamma_{kri} L_{rip}^E + L_{rip}^N)^{1+b_{kri}}, & t_{ri} > \hat{t}_{krip}. \end{cases} \tag{28}$$

In Eq. (28), when $t_{ri} > \hat{t}_{krip}$, the expression $\alpha_k^N \cdot a_{kri} \cdot (t_{ri})^{-b_{kri}} \cdot (\gamma_{kri} L_{rip}^E + L_{rip}^N)^{1+b_{kri}}$ shows that, in terms of fuel cost, 1 nm of sailing distance within ECAs is equivalent to γ_{kri} nm of sailing distance outside ECAs for $t_{ri} \in (\hat{t}_{krip}, \infty)$. Thus we call $\gamma_{kri} L_{rip}^E + L_{rip}^N$ the *converted non-ECA distance* of the path in Definition 1. An example of $g_{krip}(t_{ri})$ is shown in Figure 5.

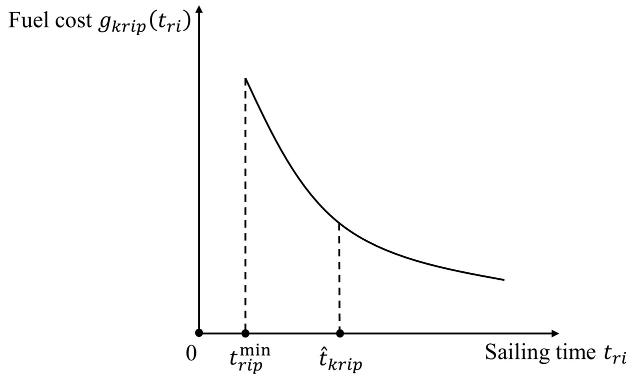

Figure 5 Curve of function $g_{krip}(t_{ri})$

Proposition 3. *The minimum fuel cost function $g_{krip}(t_{ri})$ shown in Eq. (28) is convex in t_{ri}.*

Proposition 3 shows that in the presence of only one navigable path for a leg, the minimum fuel cost is still convex, even with the speed differentiation within and outside ECAs.

4.2. Path and speed optimization model [P1] over multiple navigable paths

We now discuss the calculation of $c_{kri}(t_{ri})$ in model [P1]. Eq. (15) and Proposition 3 show that $c_{kri}(t_{ri})$ is the minimum of a set of convex functions, and we have the following proposition:

Proposition 4. *$c_{kri}(t_{ri})$ is generally non-convex and discontinuous.*

Proof. We give an example of a leg i of route r to show that $c_{kri}(t_{ri})$ can be non-convex and discontinuous. The leg has two navigable paths, path 1 and path 2. For path 1, $L_{ri1}^E = 2,000$ and $L_{ri1}^N = 18,000$. For path 2, $L_{ri2}^E = 3,000$ and $L_{ri2}^N = 16,980$. The conversion factors a_{kri} and b_{kri} are set to 7.81×10^{-4} and 2, respectively, the fuel prices α_k^E and α_k^N are 700 US\$/ton and 600 US\$/ton, respectively, and the maximum speed $V^{\max}$ is 23 knots. Then, $t_{ri1}^{\min} = 870$h and $t_{ri2}^{\min} = 869$h. It can then be calculated that $g_{kri2}(t_{ri}) > g_{kri1}(t_{ri})$ over $[t_{ri1}^{\min}, \infty)$ but only $g_{kri2}(t_{ri})$ is defined over $[t_{ri2}^{\min}, t_{ri1}^{\min})$. Therefore, $c_{kri}(t_{ri})$ is non-convex and discontinuous, as shown in Figure 6. □

Given a sailing time t_{ri}, we can calculate the fuel cost for each path p in P_{ri} with Eq. (28) and select the one with the lowest cost. For leg i of route r, we can numerically evaluate $c_{kri}(t_{ri})$ at many discretized points of sailing time t_{ri}. The results of $c_{kri}(t_{ri})$ for all legs of a route will be used in the schedule design model for the route.

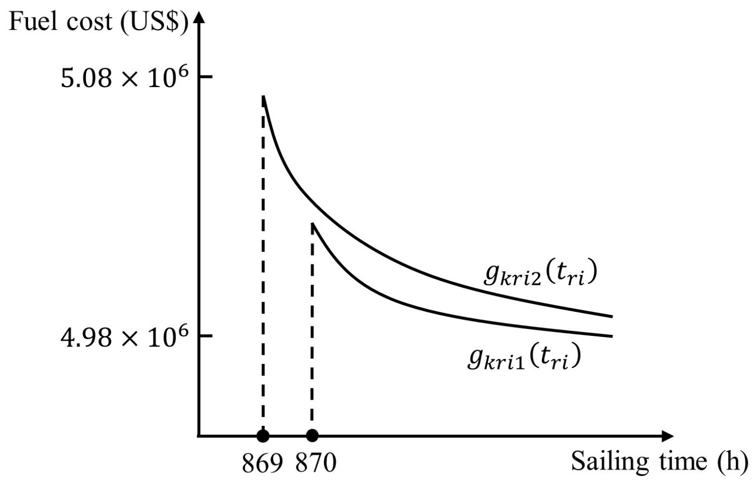

Figure 6 Fuel cost curves of two navigable paths

4.3. Minimum fuel cost functions with random port times

We have assumed that a ship spends a fixed time at each port of call. In practice, the time a ship spends at a port depends on the volume of cargo handled, the productivity of the port, and whether the port is congested, which cannot be known beforehand (Lee et al. 2015). Li et al. (2016) defined two types of uncertainties that lead to random port times: regular uncertainties, which are recurring probabilistic activities, and disruptive events, which are occasional or one-off events, and pointed out that in the tactical planning stage, regular uncertainties can be factored in. Our focus is on tactical-level liner shipping service planning, so we consider how our model can handle regular uncertainties assuming that ships must arrive at each port of call on the scheduled time even with random port times. We denote by $\tilde{\Gamma}_{ri}$ the random time spent at the ith port of call on route r. Suppose that $\tilde{\Gamma}_{ri}$ can take a total of Θ_{ri} values, denoted by $\Gamma_{ri\theta}$, $\theta = 1, ..., \Theta_{ri}$. Without loss of generality, we assume $\Gamma_{ri1} < \Gamma_{ri2} < ... < \Gamma_{ri\Theta_{ri}}$. We define $p_{ri\theta} := \Pr(\tilde{\Gamma}_{ri} = \Gamma_{ri\theta})$. $p_{ri\theta} > 0$, $\theta = 1, ..., \Theta_{ri}$, and $\sum_{\theta=1}^{\Theta_{ri}} p_{ri\theta} = 1$. We define $\bar{\Gamma}_{ri}$ as the average time a ship spends at the ith port of call on route r, that is, $\bar{\Gamma}_{ri} = \sum_{\theta=1}^{\Theta_{ri}} p_{ri\theta}\Gamma_{ri\theta}$. We denote by $\bar{t}_{ri}$ the scheduled *average* sailing time on leg i of route r. Despite the randomness of port time, the ships must provide liner shipping services, which means they have to adjust their speeds to make sure they arrive at the next port of call at the scheduled time. Therefore, when the ship leaves the ith port of call of route r, the actual time it spends at the port is observed, denoted by $\Gamma_{ri\theta}$, and the actual sailing time is $\bar{t}_{ri} + \bar{\Gamma}_{ri} - \Gamma_{ri\theta}$. To ensure the actual sailing time is at least $t_{ri}^{\min}$ under all scenarios $\theta = 1, ..., \Theta_{ri}$, we must have $\bar{t}_{ri} \geq t_{ri}^{\min} + \Gamma_{ri\Theta_{ri}} - \bar{\Gamma}_{ri}$. We define $\bar{c}_{kri}(\bar{t}_{ri})$ as the *expected* fuel costs for a ship of type $k \in K$ to sail on leg i of route r when the *average* sailing time is $\bar{t}_{ri}$. Then,

$$\bar{c}_{kri}(\bar{t}_{ri}) = \sum_{\theta=1}^{\Theta_{ri}} p_{ri\theta} \cdot c_{kri}(\bar{t}_{ri} + \bar{\Gamma}_{ri} - \Gamma_{ri\theta}), \qquad \bar{t}_{ri} \geq t_{ri}^{\min} + \Gamma_{ri\Theta_{ri}} - \bar{\Gamma}_{ri},$$

$$r=1,...,R,\ i=1,...,I_r,\ k\in K. \tag{29}$$

The values of $\bar{c}_{kri}(\bar{t}_{ri})$ can be used in place of $c_{kri}(t_{ri})$ in the schedule design and fleet deployment models. As the path and speed optimization decision of a leg is independent of the decisions for the other legs, Eqs. (29) are valid even when the random variables $\tilde{\Gamma}_{ri}$, $r=1,...,R$, $i=1,...,I_r$, are correlated.

5. Schedule design model [P2]

The fuel cost functions for legs $c_{kri}(t_{ri})$ derived in Section 4 for $k\in K_1$ and in Eq. (11) for $k\in K_2$ are the key inputs for the schedule design. Once the value of $\mathbf{m}_r$ is determined, the optimal schedule of a route r is independent of the decisions for the other routes. Therefore, the design of the schedule can be carried out for each route separately. We address model [P2] with the given $\mathbf{m}_r$ in this section.

Despite the non-convexity of $c_{kri}(t_{ri})$, the optimal schedule for a route can be obtained using dynamic programming, because given the total sailing time $W\sum_{k\in K} m_{kr}-\Gamma_r$ on all the legs, the optimal allocation of sailing time for a leg i depends only on $\sum_{i'=1}^{i-1} t_{ri'}$, i.e., the *total* sailing time allocated for legs $1,...,i-1$, rather than on $t_{ri'}$ for each of the legs $i'=1,...,i-1$. To apply dynamic programming, we discretize the sailing time for each leg into units of Δ hours (e.g., $\Delta=1$) and replace the total sailing time $W\sum_{k\in K} m_{kr}-\Gamma_r$ for the route by $\Delta\cdot\lfloor\frac{W\sum_{k\in K} m_{kr}-\Gamma_r}{\Delta}\rfloor$, where $\lfloor x\rfloor$ returns the largest integer not greater than x. Then, the dynamic programming approach has I_r stages, where the state of a stage i represents the total sailing time allocated to legs $1,...,i-1$, and the decision at a state of stage i is the sailing time t_{ri} allocated to leg i. —The details of the dynamic programming approach are presented in §EC.2. — Dear Prof Lee, since reviewer 2 said 'I consider the Appendices as not very interesting', we deleted EC.2

We define $\hat{I}:=\max_{r=1,...,R} I_r$ and $\hat{P}:=\max_{r=1,...,R,\ i=1,...,I_r}|P_{ri}|$. Then, the number of stages in the dynamic programming approach for route $r=1,...,R$ is at most $\hat{I}$, the number of states of each stage is bounded by $O\left(\frac{\sum_{k\in K} Q_k}{\Delta}\right)$, and the number of feasible decisions at each state of each stage is bounded by $O\left(\frac{\sum_{k\in K} Q_k}{\Delta}\right)$. Each decision involves the evaluation of the functions $c_{kri}(t_{ri})$ at one value of t_{ri}. For $k\in K_1$, evaluating $c_{kri}(t_{ri})$ involves calculating the fuel cost for $|P_{ri}|$ paths and calculating the fuel cost for a path requires time bounded by $O(1)$. For $k\in K_2$, $c_{kri}(t_{ri})$ can be obtained by Eq. (11). Therefore, using the dynamic programming approach, the value of $C_r(\mathbf{m}_r)$ for a given route $r=1,...,R$ and a given fleet deployment vector $\mathbf{m}_r$ can be obtained in time bounded by $O\left(\hat{I}\cdot(|K_1|\hat{P}+|K_2|)\cdot\left(\frac{\sum_{k\in K} Q_k}{\Delta}\right)^2\right)$. Given that the number of ship types $|K|$ does not increase with the size of the problem, the computational time is bounded by $O\left(\hat{I}\cdot\hat{P}\cdot\left(\frac{\sum_{k\in K} Q_k}{\Delta}\right)^2\right)$.

6. Fleet deployment model [P3]

The values of $C_r(\mathbf{m}_r)$ for all of the routes $r = 1, ..., R$ and all possible vectors $\mathbf{m}_r$ for each route r, $m_{1,r} = 0, ..., Q_1, ..., m_{|K|,r} = 0, ..., Q_{|K|}$, $\sum_{k\in K} m_{kr} \geq m_r^{\min}$, are obtained by the schedule design model [P2] and are the key inputs for the fleet deployment model [P3].

6.1. Model property

We first analyze the properties of function $C_r(\mathbf{m}_r)$. We define the convexity of a function over integer variables as discrete convexity.

Proposition 5. *The function $C_r(\mathbf{m}_r)$ is not necessarily convex or concave in any component m_{kr} of $\mathbf{m}_r$, $k \in K$.*

The intuition behind Proposition 5 is Proposition 4.

We then examine the property of $C_r(\mathbf{m}_r)$ when fixing the total number of ships $\sum_{k\in K} m_{kr}$ deployed on route r. We define $\mathbf{e}_k$ as a $|K|$-dimensional vector whose kth element is 1 and whose other elements are all 0. Then $C_r(\mathbf{m}_r)$ has the following property:

Lemma 1. *Consider a route r with m_{kr} type-k ships deployed, $k \in K$. Then, for any two ship types $k_1 \in K$, $k_2 \in K$, $k_1 \neq k_2$, if $m_{k_1 r} \geq 2$, we have $C_r(\mathbf{m}_r) - C_r(\mathbf{m}_r - \mathbf{e}_{k_1} + \mathbf{e}_{k_2}) \leq C_r(\mathbf{m}_r - \mathbf{e}_{k_1} + \mathbf{e}_{k_2}) - C_r(\mathbf{m}_r - 2\mathbf{e}_{k_1} + 2\mathbf{e}_{k_2})$.*

Lemma 1 suggests that if replacing a type-k_1 ship on route r by a type-k_2 ship can reduce fuel costs, i.e., $C_r(\mathbf{m}_r) - C_r(\mathbf{m}_r - \mathbf{e}_{k_1} + \mathbf{e}_{k_2}) > 0$, then replacing a second type-k_1 ship by a second type-k_2 ship will lead to a more significant reduction in fuel cost. Thus, the marginal fuel cost reduction by replacing a type-k_1 ship on a route by a type-k_2 ship increases as more type-k_1 ships are replaced by type-k_2 ships. The intuition is as follows: as more type-k_2 ships are deployed on route r, the optimal schedule will be more in favor of type-k_2 ships, that is, the total fuel cost for a type-k_2 ship to complete a round-trip journey of r, as shown in Eq. (1), will be lower. Thus, the marginal fuel cost reduction by replacing a type-k_1 ship on a route by a type-k_2 ship increases as more type-k_1 ships are replaced.

Based on Lemma 1, we have the following theorem:

Theorem 1. *The fleet deployment model [P3] has an optimal solution, denoted by $\mathbf{m}^*$, in which any two routes have at most one common type of ship deployed. Thus, there does not exist two routes $r_1, r_2 = 1, ..., R$, $r_1 \neq r_2$ and two types of ships $k_1, k_2 \in K$, $k_1 \neq k_2$ such that $m^*_{k_1,r_1} \geq 1$, $m^*_{k_2,r_1} \geq 1$, $m^*_{k_1,r_2} \geq 1$, and $m^*_{k_2,r_2} \geq 1$.*

The managerial insight of Theorem 1 is that deploying multiple types of ships on one route is generally undesirable. The rationale is that different types of ships deployed on the same route have to compromise to follow the same schedule. The intuition behind Theorem 1 can be understood by the following corollary and example.

Corollary 1. *If $|K|=2$ in the fleet deployment model [P3], then there exists an optimal solution in which at most one route has both types of ships deployed and each of the other routes has only one type of ship deployed.*

Corollary 1 can be illustrated by the following example.

Example 1. Suppose that there are two types of ships: traditional ships and scrubber-equipped ships. Suppose that routes 1 and 2 have the same sequence of ports of call. All legs have the same fuel consumption rate functions: $a_{kri}=a$ and $b_{kri}=b$ for $k=1,2$, $r=1,2$, $i\in I_r$. Consider two fleet deployment options: in option A, both route 1 and route 2 have three traditional ships and three scrubber-equipped ships deployed; in option B, six traditional ships are deployed on route 1 and six scrubber-equipped ships on route 2. Then in option B, all ships on route 1 sail at lower speeds on legs that are fully covered by ECAs and at higher speeds on legs that are not covered by ECAs, and all ships on route 2 sail at a constant speed on all of the legs. In contrast, in option A, the two types of ships have to follow the same schedule and thus the fuel costs in option A are higher than those in option B.

6.2. Pseudo-polynomial time algorithm

To solve model [P3], we enumerate all possible fleet deployment decisions for each route $r=1,...,R$, i.e., all possible combinations of $m_{1,r}=0,...,Q_1,...,m_{|K|,r}=0,...,Q_{|K|}$, $\sum_{k\in K} m_{kr}\ge m_r^{\min}$, and solve the schedule design model [P2] for each r and each $\mathbf{m}_r$. The results are used as inputs for model [P3].

We note that the optimal fleet deployment for a route r depends on the *total* number of ships of each type deployed on the other routes, rather than the number of ships of each type deployed on each of the other routes. Based on this property, we design a dynamic programming algorithm. We define $f(s,q_1,...,q_{|K|})$, $s=1,...,R$, and $q_k=0,...,Q_k$, $k\in K$ as the minimum total average cost per week of routes $1,...,s$ when a total of q_k ships of type $k\in K$ can be deployed on them (not all ships must be used). Then, $f(s,q_1,...,q_{|K|})$ has the recursive relation

$$f(s,q_1,...,q_{|K|})= \min_{\substack{m_{1,s}=0,...,q_1\\ \cdots \\ m_{|K|,s}=0,...,q_{|K|}\\ \sum_{k\in K} m_{ks}\ge m_s^{\min}}} \left[\sum_{k\in K} c_k\cdot m_{ks}+C_s(m_{1,s},...,m_{|K|,s})+f(s-1,q_1-m_{1,s},...,q_{|K|}-m_{|K|,s})\right], \tag{30}$$

$$s=2,...,R,\ q_1=0,...,Q_1,\ ...,\ q_{|K|}=0,...,Q_{|K|},\ \sum_{k\in K} q_k\ge\sum_{s'=1}^{s} m_{s'}^{\min} \tag{31}$$

and the boundary conditions are

$$f(1,q_1,...,q_{|K|})= \min_{\substack{m_{1,1}=0,...,q_1\\ \cdots \\ m_{|K|,1}=0,...,q_{|K|}\\ \sum_{k\in K} m_{k,1}\ge m_1^{\min}}} \left[\sum_{k\in K} c_k\cdot m_{k,1}+C_1(m_{1,1},...,m_{|K|,1})\right], \tag{32}$$

$$q_1 = 0, ..., Q_1, ..., q_{|K|} = 0, ..., Q_{|K|}, \quad \sum_{k \in K} q_k \geq m_1^{\min}. \tag{33}$$

We aim to obtain $f(R, Q_1, ..., Q_{|K|})$. To this end, we must try all the values of s in $\{1, ..., R\}$ and q_k in $\{0, ..., Q_k\}$, $k \in K$. For each combination $(s, q_1, ..., q_{|K|})$, we need to evaluate at most $\prod_{k\in K}(Q_k + 1)$ decisions. Therefore, the fleet deployment problem can be solved in time bounded by $O\left(R \cdot \left(\prod_{k\in K}(Q_k+1)\right)^2\right)$, which is equivalent to the complexity of $O\left(R \cdot \left(\prod_{k\in K} Q_k\right)^2\right)$ (note that the number of ship types $|K|$ does not increase with the size of the problem).

Proposition 6. *Given the known values of $C_r(\mathbf{m}_r)$, $r = 1, ..., R$, $m_{1,r} = 0, ..., Q_1$, ..., $m_{|K|,r} = 0, ..., Q_{|K|}$, $\sum_{k\in K} m_{kr} \geq m_r^{\min}$, the fleet deployment problem [P3] can be solved in time bounded by $O\left(R \cdot \left(\prod_{k\in K} Q_k\right)^2\right)$, which is pseudo-polynomial in complexity.*

Our problem [P3] nests the multiple-choice knapsack problem (Pisinger 1995) as a special case. This problem is known to be NP-hard, and the best known algorithm for finding an optimal solution requires pseudo-polynomial computation time. Our algorithm for [P3] is also pseudo-polynomial.

6.3. Extension to fleet deployment with ship retrofitting

We can extend the fleet deployment model [P3] to consider retrofitting traditional ships with scrubbers (converting a traditional ship into a scrubber-equipped ship). Let $k' \in K$ be a particular type of ship that can be converted to another type of ship denoted by $k'' \in K$ at a retrofitting cost U. The retrofitting cost U occurs once. As we use weekly costs in the calculation, we convert the retrofitting cost U into an equivalent weekly cost, denoted by u. The company must decide the number of type-k' ships to convert into type-k'' ships, denoted by $y \in \mathbb{Z}_+$, and the numbers of ships of each type $k \in K$ to deploy on the routes after the conversion. This problem can be formulated as model [P3']:

$$\text{[P3']} \quad \min \quad u \cdot y + \sum_{r=1}^{R} \left[\sum_{k\in K} c_k \cdot m_{kr} + C_r(\mathbf{m}_r) \right] \tag{34}$$

subject to

$$\sum_{r=1}^{R} m_{k'r} \leq Q_{k'} - y \tag{35}$$

$$\sum_{r=1}^{R} m_{k'',r} \leq Q_{k''} + y \tag{36}$$

$$\sum_{r=1}^{R} m_{kr} \leq Q_k, \quad k \in K \setminus \{k', k''\} \tag{37}$$

$$\sum_{k\in K} m_{kr} \geq m_r^{\min}, \quad r = 1, ..., R \tag{38}$$

$$m_{kr} \in \mathbb{Z}_+, \quad r = 1, ..., R, \ k \in K \tag{39}$$

$$y \in \mathbb{Z}_+. \tag{40}$$

Based on Lemma 1, we prove that problem [P3'] has the following nice property:

Proposition 7. *If the optimal value of y in [P3'] is greater than 0, there exists an optimal solution in which no route has both type-k' and type-k'' of ships deployed.*

The rationale behind Proposition 7 is as follows. If in an optimal solution a route $\hat{r}$ has both types of ships deployed, one of its type-k'' ships deployed can be considered as a newly retrofitted ship because the optimal value of y is greater than 0. Thus, it is worthwhile retrofitting a type-k' ship on route $\hat{r}$. Then Lemma 1 implies it is worthwhile retrofitting all type-k' ships on route $\hat{r}$.

7. Numerical experiments

This section reports the computational results of randomly generated instances based on realistic parameter settings. A laptop computer (Intel Core i7, 2.5GHz; Memory, 8G) is used to conduct these experiments with the programming language C# (Visual Studio 2012).

7.1. Computational time of the nesting algorithmic framework

We first report the computational time of the proposed nesting algorithmic framework. The testing instances are generated as follows. We investigate three experimental groups with different numbers of liner routes $R \in \{10, 20, 30\}$ involving the North Sea, the North America, and the United States Caribbean Sea ECAs. The boundaries of the ECAs are given in IMO (2019). Each experimental group comprises five test instances, and each instance has a different number of ports of call, which are selected from real ports within or outside ECAs. For a leg covering ECAs, we will discretize the boundaries of the ECAs into intervals of 10 nm and treat each discretization point as a candidate location for crossing the ECA boundaries. The navigable paths of the leg can be constructed as shown in Figure 3. The paths with longer total sailing distances and longer distances within ECAs than others will be removed, and the remaining paths comprise the path set of the leg. For a leg without ECAs, the path set contains only its shortest path. We assume all sailing paths are navigable. The time spent at each port of call is randomly generated and is between 12 hours and 60 hours (Qi and Song 2012). Suppose that ships with the capacity of 18,000 20-ft containers (TEUs) will be deployed on the routes. The maximum speed of these ships is set to 23 knots (Seatrade-ShipTech-Middle-East 2019). The ships are divided into two types: traditional ships (type 1) and scrubber-equipped ships (type 2). The total number of ships of the two types is generated based on the roundtrip journey distances of the routes and the maximum speed of the ships. Specifically, $\sum_{k=1}^{2} Q_k$ is obtained by a uniform distribution $(\sum_{r=1}^{R} m_r^{\min} \times 1.1, \sum_{r=1}^{R} m_r^{\min} \times 2)$. The number of ships of type 1, i.e., Q_1, is randomly generated between 1 and $\sum_{k=1}^{2} Q_k$, and Q_2 is produced by $\left(\sum_{k=1}^{2} Q_k\right) - Q_1$. The fixed costs of a traditional 18,000-TEU ship and a scrubber-equipped ship are set to 271,700 US$/week and 283,500 US$/week, respectively (MI-News-Network 2017, Gu and Wallace 2017, Seatrade-ShipTech-Middle-East 2019). Referring to MI-News-Network (2017), the conversion factors a_{kri} and b_{kri} between fuel consumption rate and sailing speed for an 18,000-TEU ship are set to 7.81×10^{-4} and 2, respectively, for both types of ships and all legs of all routes. The 0.5% global sulfur limit put into force from 1 January 2020 may cause the fluctuation of fuel prices, while the outbreak of novel coronavirus since early 2020 also has a significant impact on bunker prices. It is difficult to find representative prices, i.e., the fuel prices have not been influenced by the COVID-19 crises, after the implementation of the new global sulfur limit. Therefore, we will set the fuel prices based on the data in late 2019, and some sensitivity analyses on fuel prices will be conducted in Section 7.4. According to the global average fuel prices from October to December in 2019 (**?**), the prices of HSFO, VLSFO and MGO are set to 410 US$/ton, 600 US$/ton and 700 US$/ton, respectively.

Each instance is solved by the nesting algorithmic framework to obtain the optimal solution through the following process. We use the algorithms in Section 5 to design the optimal schedule for each route with given numbers of the two types of ships deployed ($\Delta = 1$). Then, the dynamic programming-based pseudo-polynomial time algorithm is applied to assign ships to the routes. The optimal objective value ("OBJ_{ECA}") and the computation time ("CPU time") for the three groups of test instances are reported in Table 1.

7.2. Effectiveness of the proposed integrated model considering ECAs

To test the effectiveness of the proposed integrated model, we solve each instance without considering ECAs and compare the resulting solutions with the optimal ones for the integrated model. —The solutions without considering ECAs are obtained by the algorithm in §EC.3. — Dear Prof Lee, since reviewer 2 said 'I consider the Appendices as not very interesting', we deleted EC.3 The comparison between the solutions considering and not considering ECAs for the three groups of instances is reported in the "Gap" column of Table 1. This shows that considering ECAs in service planning can reduce over 2% of the costs. As the *annual* operating cost of a shipping company's network can be as high as several billion dollars, a 2% cost saving is significant for these companies. Therefore, the proposed model considering ECAs will be of benefit to liner shipping operations management.

7.3. Performance for speed optimization for comment 1-13

We have investigated the effectiveness of the proposed model considering ECAs, where the path and speed optimization makes a significant contribution on cost savings. It is interesting to further analyze the performance of speed optimization only. For each instance, we will choose the shortest paths for all routes first and then generate the solution by optimizing the speed, schedule and fleet deployment considering ECAs (called solution not optimizing path). Comparing between the solutions not optimizing path and not considering ECAs, we can obtain the cost savings that come from speed optimization. We can see the computational results in Table 1.

Table 1 **Computational time of the nesting algorithmic framework and comparison between solutions**

Instances	Consider ECAs		Not consider ECAs		Not optimize path	
	OBJ_{ECA}	CPU time (s)	OBJ_{NECA}	Gap_1	$\text{OBJ}_{\text{Npath}}$	Gap_2
10-1						
10-2						
10-3						
10-4						
10-5						
20-1						
20-2						
20-3						
20-4						
20-5						
30-1						
30-2						
30-3						
30-4						
30-5						

Notes:
(i) Instance "10-1" means the first instance of the group of 10 routes.
(ii) "OBJ_{ECA}" is the total average cost per week of the optimal decisions considering ECAs, "OBJ_{NECA}" is the total average cost per week of the decisions without considering ECAs, and "$\text{OBJ}_{\text{Npath}}$" is the total average cost per week of the decisions without optimizing path.
(iii) "Gap_1" is calculated as $(\text{OBJ}_{\text{NECA}} - \text{OBJ}_{\text{ECA}})/\text{OBJ}_{\text{ECA}}$ and "Gap_2" is calculated as $(\text{OBJ}_{\text{NECA}} - \text{OBJ}_{\text{Npath}})/\text{OBJ}_{\text{Npath}}$.

7.4. Sensitivity with fuel price for comments 1-2 and 2-2

The prices of MGO, VLSFO and HSFO have fallen sharply since January 2020. Considering the uncertainty of fuel price, we analyze the sensitivity of the gaps for the first five instances in Table 1 with the decrease of fuel prices to further validate the effectiveness of the proposed model. Based on the global average bunker prices in the first four months of 2020, we design six groups of fuel prices on MGO, VLSFO and HSFO. A figure similar with Figure 7 will be reported here.

7.5. Sensitivity with the fixed cost of scrubber-equipped ships for comment 1-14

The fixed cost of a scrubber-equipped ship is set to be 11,800 US$/week (283,500 minus 271,700 US$/week) higher than that of a traditional ship in the experiments in Sections 7.1 and 7.2. The cost of scrubbers is expected to decrease with the maturity of technology and economy of scale, due to their wider adoption. Therefore, we examine the effectiveness of the integrated model considering

Table 2 Prices of MGO, VLSFO and HSFO

Groups	MGO	VLSFO	HSFO
1	395	265	200
2	460	345	240
3	525	425	280
4	590	505	320
5	655	585	360
6	720	665	400

ECAs when the fixed cost of scrubber-equipped ships decreases. We test the first five instances in Table 1. For each instance, we set the fixed cost (c_2) of a scrubber-equipped ship at a value from 283,500 (11,800 US$/week higher than that of a traditional ship), 282,320 (90%×11,800 US$/week higher), 281,140, 279,960, 278,780, and 277,600 (50%×11,800 US$/week higher) US$/week. We study two cases as follows: when the total number of available ships is less than or equal to the total optimal number of ships deployed on all routes (case 1), we report the gaps between the total costs considering ECAs and those without considering ECAs for the five instances with 10 routes shown in Figure 7 by solid lines; when the total number of available ships is more than the total optimal number of ships deployed on all routes (case 2), the gaps for the five instances are shown with dotted lines in Figure 7. The figure indicates that the cost savings brought by the integrated model are still significant even when the fixed costs of scrubber-equipped ships significantly decrease. In case 1, all ships will be deployed on routes. With the decrease of the fixed cost of scrubber-equipped ship, the optimal solution on path and speed, schedule design and fleet deployment is constant, and the decrease of the total cost considering ECAs will lead to the slightly increase of the gap between the total costs considering and not considering ECAs. In case 2, ***

7.6. Effect of ECAs on fleet deployment for comment 1-15

We will analyze the solutions on fleet deployment when ECAs are considered and not considered. The number and type of ships deployed on each route for the first instance in Table 1 are reported in Table 3.

8. Conclusions

In this study we explore a sustainable liner shipping operations management problem. We address holistic liner shipping service planning that integrates fleet deployment, schedule design, and ship routing, considering the effect of ECAs. The objective is to minimize the costs for liner shipping companies while complying with the ECA rules. The interlinked decisions of fleet deployment, schedule design, and ship routing and the ECA regulations complicate the problem. We propose a nesting algorithmic framework to address this new and challenging problem. In our

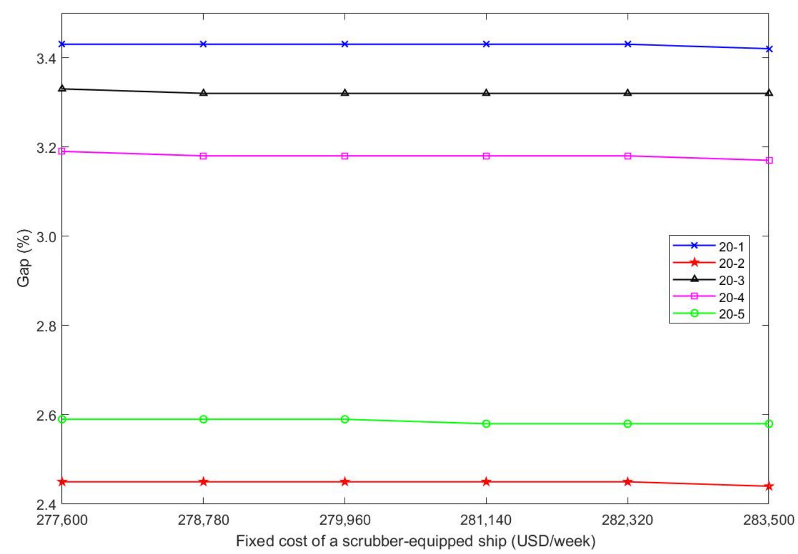

Figure 7 **Sensitivity of the gaps between considering ECAs and not considering ECAs with the fixed cost of a scrubber-equipped ship**

Table 3 **Number and type of ships deployed in the solutions considering and not considering ECAs**

Routes	Consider ECAs		Not consider ECAs	
	Type 1	Type 2	Type 1	Type 2
1				
2				
3				
4				
5				
6				

theoretical analysis of the framework, we find that the minimum fuel cost of a ship on a leg is generally not convex in the sailing time (Proposition 4) and the minimum fuel cost of a route is not necessarily convex or concave in the number of ships deployed (Proposition 5). We show that deploying multiple types of ships on one route is generally undesirable because different types of ships have to compromise to follow the same schedule (Theorem 1 and Corollary 1). We prove that the fleet deployment problem with multiple types of ships can be solved in pseudo-polynomial time (Proposition 6). When considering retrofitting traditional ships with scrubbers, we prove either all traditional ships on a route should be converted into scrubber-equipped ships or no traditional ship should be converted (Proposition 7). Extensive numerical experiments are conducted to validate the effectiveness of the proposed models. The computational results show that considering the effect of ECAs in liner shipping operations management can reduce over 2% of the costs. In addition, the computation time for instances with 60 routes does not exceed three hours.

References

Abadie LM, Goicoechea N, Galarraga I (2017) Adapting the shipping sector to stricter emissions regulations: Fuel switching or installing a scrubber? *Transportation Research Part D: Transport and Environment* 57:237–250.

Angelus A, Zhu W (2017) Looking upstream: Optimal policies for a class of capacitated multi-stage inventory systems. *Production and Operations Management* 26(11):2071–2088.

Baldacci R, Battarra M, Vigo D (2008) Routing a heterogeneous fleet of vehicles. *The Vehicle Routing Problem: Latest Advances and New Challenges*, 3–27.

Bockmann MW (2020) Dry bulk and containerships lead 'flood' of scrubber cancellations. URL `https://lloydslist.maritimeintelligence.informa.com/LL1131688/Dry-bulk-and-containerships-lead-flood-of-scrubber-cancellations`, (Accessed on 1 May 2020).

Chen H, Solak S (2015) Lower cost arrivals for airlines: Optimal policies for managing runway operations under optimized profile descent. *Production and Operations Management* 24(3):402–420.

Chong KC, Henderson SG, Lewis ME (2015) The vehicle mix decision in emergency medical service systems. *Manufacturing & Service Operations Management* 18(3):347–360.

Christiansen M, Fagerholt K, Nygreen B, Ronen D (2013) Ship routing and scheduling in the new millennium. *European Journal of Operational Research* 228(3):467–478.

Christiansen M, Fagerholt K, Ronen D (2004) Ship routing and scheduling: Status and perspectives. *Transportation Science* 38(1):1–18.

Cordeau JF, Toth P, Vigo D (1998) A survey of optimization models for train routing and scheduling. *Transportation science* 32(4):380–404.

Doudnikoff M, Lacoste R (2014) Effect of a speed reduction of containerships in response to higher energy costs in sulphur emission control areas. *Transportation Research Part D: Transport and Environment* 28:51–61.

European Maritime Safety Agency (2017) Sulphur directive. Http://www.emsa.europa.eu/main/air-pollution/sulphur-directive.html. Accessed 24 June 2017.

Fagerholt K, Gausel NT, Rakke JG, Psaraftis HN (2015) Maritime routing and speed optimization with emission control areas. *Transportation Research Part C: Emerging Technologies* 52:57–73.

Fagerholt K, Laporte G, Norstad I (2010) Reducing fuel emissions by optimizing speed on shipping routes. *Journal of the Operational Research Society* 61(3):523–529.

Fagerholt K, Psaraftis HN (2015) On two speed optimization problems for ships that sail in and out of emission control areas. *Transportation Research Part D: Transport and Environment* 39:56–64.

Fransoo JC, Lee CY (2013) The critical role of ocean container transport in global supply chain performance. *Production and Operations Management* 22(2):253–268.

Gu Y, Wallace SW (2017) Scrubber: A potentially overestimated compliance method for the emission control areas: The importance of involving a ship's sailing pattern in the evaluation. *Transportation Research Part D: Transport and Environment* 55:51–66.

Hand M (2015) Maersk still concerned over non-compliance with 0.1% sulphur ECA. Http://www.seatrade-maritime.com/news/europe/maersk-still-concerned-over-non-compliance-with-01-sulphur-eca.html. Accessed 22 May 2019.

Hong Kong Environmental Protection Department (2017) A guide to the air pollution control regulation. Http://www.epd.gov.hk/epd/english/top.html. Accessed 22 May 2017.

Hvattum LM, Norstad I, Fagerholt K, Laporte G (2013) Analysis of an exact algorithm for the vessel speed optimization problem. *Networks* 62(2):132–135.

IMO (2019) International Maritime Organization. Http://www.imo.org/en/Pages/Default.aspx. Accessed 22 May 2019.

Jiang L, Kronbak J, Christensen LP (2014) The costs and benefits of sulphur reduction measures: Sulphur scrubbers versus marine gas oil. *Transportation Research Part D: Transport and Environment* 28:19–27.

Lee CY, Lee HL, Zhang J (2015) The impact of slow ocean steaming on delivery reliability and fuel consumption. *Transportation Research Part E: Logistics and Transportation Review* 76:176–190.

Lee CY, Song DP (2017) Ocean container transport in global supply chains: Overview and research opportunities. *Transportation Research Part B: Methodological* 95:442–474.

Legros B, Bouchery Y, Fransoo J (2019) A time-based policy for empty container management by consignees. *Production and Operations Management* doi: 10.1111/poms.12996.

Li C, Qi X, Song D (2016) Real-time schedule recovery in liner shipping service with regular uncertainties and disruption events. *Transportation Research Part B: Methodological* 93:762–788.

Lo HK, McCord MR (1998) Adaptive ship routing through stochastic ocean currents: General formulations and empirical results. *Transportation Research Part A: Policy and Practice* 32(7):547–561.

Maersk (2017) Maersk's ocean segment revenue in FY 2012 and FY 2018. Https://www.statista.com/statistics/326014/revenue-of-maersk-line/. Accessed 22 May 2019.

Mak HY, Rong Y, Shen ZJM (2013) Infrastructure planning for electric vehicles with battery swapping. *Management Science* 59(7):1557–1575.

Maritime and Port Authority of Singapore (2016) Extension and enhancement to the maritime Singapore green initiative. Https://www.mpa.gov.sg/web/portal/home/media-centre/news-releases/detail/271360c6-fd43-472e-b122-0d1338d0d97d. Accessed 22 May 2017.

Meng Q, Wang S, Andersson H, Thun K (2014) Containership routing and scheduling in liner shipping: Overview and future research directions. *Transportation Science* 48(2):265–280.

Meng Q, Wang T (2011) A scenario-based dynamic programming model for multi-period liner ship fleet planning. *Transportation Research Part E: Logistics and Transportation Review* 47(4):401–413.

MI-News-Network (2017) Maersk Triple-E vessels: Why size matters? Https://www.marineinsight.com/shipping-news/size-matters/. Accessed 16 July 2019.

Ng MW (2014) Distribution-free vessel deployment for liner shipping. *European Journal of Operational Research* 238(3):858–862.

Notteboom TE, Vernimmen B (2009) The effect of high fuel costs on liner service configuration in container shipping. *Journal of Transport Geography* 17(5):325–337.

Papadakis NA, Perakis AN (1990) Deterministic minimal time vessel routing. *Operations Research* 38(3):426–438.

Papageorgiou DJ, Keha AB, Nemhauser GL, Sokol J (2014) Two-stage decomposition algorithms for single product maritime inventory routing. *INFORMS Journal on Computing* 26(4):825–847.

Park JH, Kazaz B, Webster S (2018) Surface vs. air shipment of humanitarian goods under demand uncertainty. *Production and Operations Management* 27(5):928–948.

Perakis AN, Papadakis NA (1989) Minimal time vessel routing in a time-dependent environment. *Transportation Science* 23(4):266–276.

Pisinger D (1995) A minimal algorithm for the multiple-choice knapsack problem. *European Journal of Operational Research* 83(2):394–410.

Qi X, Song DP (2012) Minimizing fuel emissions by optimizing vessel schedules in liner shipping with uncertain port times. *Transportation Research Part E: Logistics and Transportation Review* 48(4):863–880.

Ronen D (2011) The effect of oil price on containership speed and fleet size. *Journal of the Operational Research Society* 62(1):211–216.

Seatrade-ShipTech-Middle-East (2019) Triple-E class container ships. Https://www.ship-technology.com/projects/triple-e-class/. Accessed 16 July 2019.

UNCTAD (2018) *Review of Maritime Transportation 2018* (New York and Geneva: Paper presented at the United Nations Conference on Trade and Development), https://unctad.org/en/PublicationsLibrary/rmt2018_en.pdf. Accessed 22 May 2019.

UNCTAD (2019) *Review of Maritime Transportation 2019* (New York and Geneva: Paper presented at the United Nations Conference on Trade and Development), https://unctad.org/en/PublicationsLibrary/rmt2019_en.pdf. Accessed 2 May 2020.

Wang S (2016) Fundamental properties and pseudo-polynomial-time algorithm for network containership sailing speed optimization. *European Journal of Operational Research* 250(1):46–55.

Wang S, Meng Q (2012) Sailing speed optimization for container ships in a liner shipping network. *Transportation Research Part E: Logistics and Transportation Review* 48(3):701–714.

Wang S, Wang X (2016) A polynomial-time algorithm for sailing speed optimization with containership resource sharing. *Transportation Research Part B: Methodological* 93:394–405.

Zis T, Angeloudis P, Bell MGH, Psaraftis HN (2016) Payback period for emissions abatement alternatives: Role of regulation and fuel prices. *Transportation Research Record: Journal of the Transportation Research Board* 2549:37–44.

Zis T, Psaraftis HN (2019) Operational measures to mitigate and reverse the potential modal shifts due to environmental legislation. *Maritime Policy & Management* 46(1):117–132.